



# COMPUTER MODELING OF A SMALL NEON GAS-PUFF Z-PINCH

Jiří Ullschmied

*Institute of Plasma Physics, Czech Academy of Sciences  
P.O. Box 17, 182 00 Prague 8, Czech Republic*

## Abstract

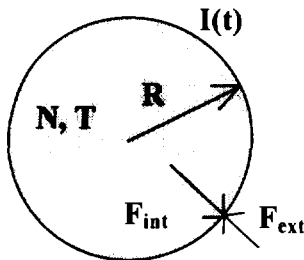
The macroscopic dynamics of a cylindrical gas-puff pinch and conditions of radiation plasma collapse are studied by using a one-dimensional ('mechanical') computer model. Besides the Joule plasma heating, compressional heating, magnetic field freezing in a plasma and recombination losses also the real temperature- and density-dependencies of radiation plasma loss are taken into account. The results of calculations are compared with experimental data taken from a small neon-puff z-pinch experiment operated at IPP Prague.

## Introduction

Pronounced radial oscillations of the beam-heated magnetized plasma column and quasi periodical bounces of the z-pinch plasma bulk radius are often observed in relativistic electron beam-plasma experiments with short-pulse beams and in small gas-puff pinches [1,2]. These oscillatory movements are in fact the forced macroscopic oscillations of an elastic hot-plasma body driven by fast changes of the radial pressure balance. In gas-puff Z-pinches, the driving force  $F_{ext}$  of plasma oscillations is the external magnetic pressure produced by the driving current  $I(t)$ , and the counter force is the plasma kinetic pressure (+ eventually the pressure of a magnetic field frozen in a plasma at early pinch stages). The pinch dynamics can be studied by using the one-dimensional analytical model (see [3-6]) based on energy, momentum and particle conservation laws, in which a long cylindrical plasma body is characterized by the (reduced) mass per unit length  $M^*=M/2$ , by the time-dependent radius  $R(t)$ , and by the (averaged over the plasma cross section) temperature  $T(t)$  and density  $N=N(t)$ .

## Model equations

Providing that the total number of particles per unit plasma length remains conserved during the investigated process), the radial plasma dynamics may be described by three coupled balance equations for three time-dependent functions only -  $R(t)$ ,  $N(t)$  and  $T(t)$  - with the initial values  $R_o, N_o, T_o$ : the particle balance equation



$$N \cdot R^2 = N_o \cdot R_o^2,$$

the momentum balance differential equation

$$M^* \cdot \frac{d^2 R}{dt^2} + c_{visc} \frac{1}{R} \frac{dR}{dt} = F_{int} - F_{ext},$$

and the energy balance differential equation

$$\frac{d}{dt} (W_{kin} + Q_{int}) = P_{heating} - P_{loss},$$

where  $F_{int} = F_{thermal} + (F_{frozen B})$  and  $F_{ext} = F_{driving I}$  are the internal forces and external (driving) forces, respectively,  $c_{visc}$  characterizes the viscous damping, and

$$F_{thermal} = NTS, \quad F_{frozen B} = \frac{\mu_o I_{st}^2}{8\pi R}, \quad F_{driving I} = \frac{\mu_o I(t)^2}{4\pi R},$$

$I(t)$  is the time-dependent driving current,  $I_{st}$  some start skin-off current value.  $P_{heating}$  is the

heating power,  $P_{\text{heating}} = P_{\text{Joule}} + P_{\text{compr}}$ , and  $P_{\text{loss}} = P_{\text{rec}} + P_{\text{radiation}}$  the loss power, where

$$P_{\text{Joule}} = \frac{1}{\sigma} \frac{I^2}{\pi R^2} \quad P_{\text{compr}} \sim M^* \frac{1}{R} \left( \frac{dR}{dt} \right)^2 \quad P_{\text{rec}} = \beta T$$

and the kinetic and thermal plasma energies  $W_{\text{kin}}$  and  $Q_{\text{int}}$  are defined as

$$W_{\text{kin}} = \frac{M^*}{2} \left( \frac{dR}{dt} \right)^2 \quad \text{and} \quad Q_{\text{int}} = 2\pi N_o \cdot R_o \cdot \frac{T}{R}$$

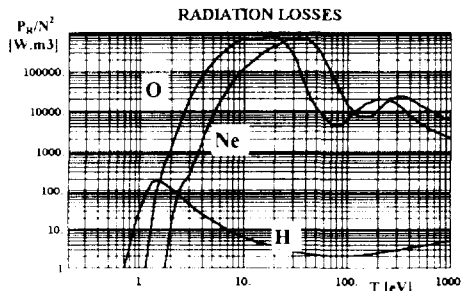


Fig. 1b

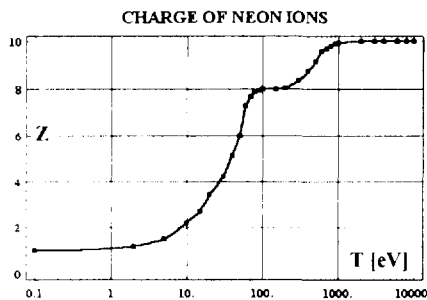


Fig. 1a

The radiation loss temperature-dependence

$$P_{\text{radiation}} \sim f_{\text{approx}}(T) \cdot N_o^2 \cdot R_o$$

is introduced through the interpolating functions (Fig. 1a) constructed on the base of the plasma radiation data for hydrogen, oxygen and neon published e.g. in [7-9].

Another approximation function is used for the temperature dependence of the neon ion charge  $Z = Z(T)$  - see Fig.1b. In such a case the substitution  $N \rightarrow N(1+Z\{T\})$  was used.

Though such an approach results in restricting the investigated plasma movement to homogenous expansion (compression) only, all plasma mixing processes (instabilities, turbulence) being necessarily neglected, it proved to be useful at studying the influence on the global plasma dynamics of a number of energy transfer processes. On the first place the influence of radiation losses on the pinch dynamics was studied.

### Pinch dynamics without radiation losses

The simplest case of undamped plasma bouncing at a constant driving current and negligible losses may be handled analytically. For a constant fully skinned-out driving current  $I_o$ , the period of oscillations is (in the first approximation) proportional to the square root of  $M^*/I_o^2$ , and the minimum plasma radius is proportional to  $N_o T_o R_o^3 / I_o^2$ . The time of the first plasma compression does not differ much from the time of singularity of the solution for an infinitely thin hollow plasma cylinder of equivalent mass (zero counter force) - c.f the gray line in Fig. 2a.

In all other cases Wolfram's Mathematica was used for solving the balance equations numerically. When neglecting completely the Joule heating and radiation losses, the plasma radius oscillates around the Bennet equilibrium. The full curve in Fig.2a shows the bouncing calculated for a constant driving current and small recombination losses only. The time dependencies the total energy  $W$ , and of the kinetic and thermal energy components are depicted in Fig. 2b.

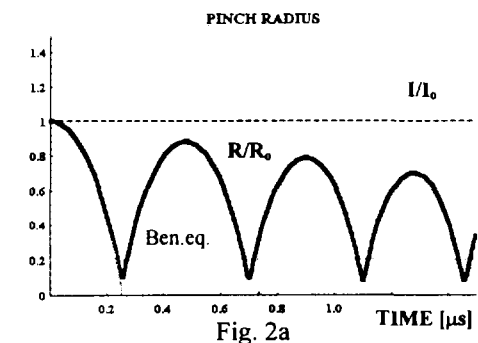


Fig. 2a

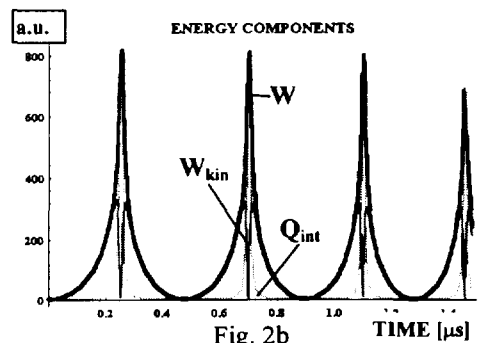


Fig. 2b

The dynamics of the pinch radius calculated for a sinusoidal driving current with  $I_{\max}=160$  kA and no radiation losses is shown in Fig. 3a, and the corresponding dependence of the plasma temperature in Fig. 3b.

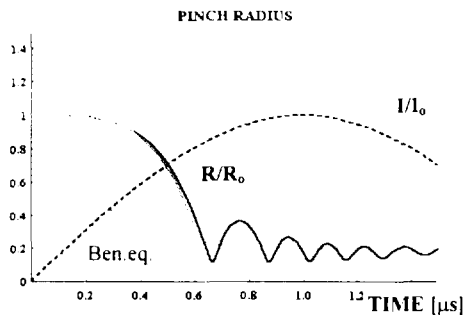


Fig. 3a

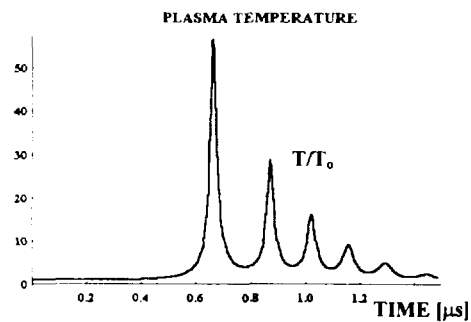


Fig. 3b

### Pinch dynamics without radiation losses

As soon as the radiation losses are taken into account, neither the Joule, nor the compressional heating (even when taking into account the frozen-in magnetic field) manages to stop the radiation collapse (the solution has a singularity with  $R \rightarrow 0$ ). Radiation collapse can be avoided e.g. by assuming that the plasma column gradually becomes optically thick, so that at the moment of maximum compression the radiation comes from a thin surface layer only, the thickness of which is proportional to the current plasma radius. The pinching then stops at the radius, at which the energy input and output become balanced (around  $R/R_0 = 0.1$ ,  $T/T_0 \approx 15$  - see the full lines in Figs. 4a, b).

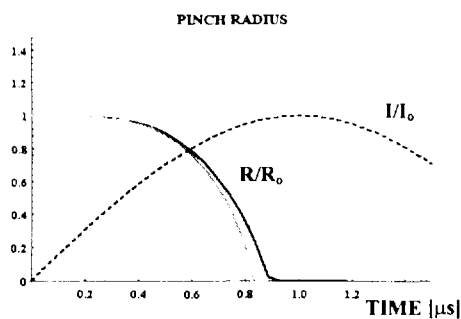


Fig. 4a

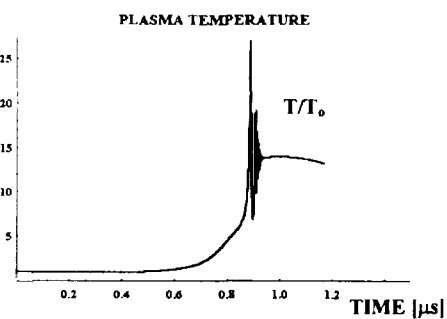


Fig. 4b

Most of the calculations were tailored to the small IPP neon gas-puff pinch ( $I_{\max}=160$  kA,  $N_0=10^{17}$  cm $^{-3}$ ,  $R_0=1$  cm,  $T_0=1$  eV) - [12]. The calculated minimum plasma radius  $R_{\min} \approx 0.6$  mm, the maximum temperature of the plasma bulk  $T_{\max} \approx 60$  eV, and the maximum plasma density  $N_{\max} \approx 2.5 \cdot 10^{19}$  cm $^{-3}$  at the main plasma compression stage agree remarkably well with the experimentally obtained values.

### Radiated power

Also the calculated time dependence of the radiated XUV power resembles well the experimental one. The simulated curves make it possible to explain all the main features of the observed XUV signals, namely the repeated bouncing observed at non-optimum pinch parameters, and pronounced splitting of the radiation peak corresponding to the first plasma compression - see Fig. 5. The computed time

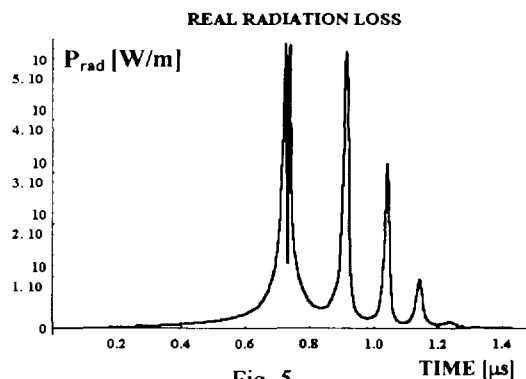


Fig. 5

dependences of the radiation losses agree qualitatively well with the measured XUV signals even at the times after the first plasma compression. In particular, in non-optimum pinch regimes the split broad first radiation peak is followed by several narrower spikes with a comparable or lower amplitude.

At the optimum pinching, however, strong MHD instabilities developing during the first compression (witnessed e.g. by the occurrence of hot spots [10]) result in and a partial or even total current disruption, some part of the current being expelled to the peripheral discharge regions.

The disruption process was simulated in a model way by changing the time dependence of the driving current  $I(t)$  several tens of ns after the maximum pinching. The temporal dependence of the radiated power after the maximum plasma compression on a longer time scale is determined by the time delay and by the speed of the current disruption. At a fast current disruption the radiation signal turns to a single split peak. If the current disruption is only temporal (see Fig. 6a) another much narrower radiation peak may occur several hundred ns after the first compression, as shown in Fig. 6b. At a slower but irreversible current disruption (see Fig 7a) the radiation signal decay becomes slower - Fig. 7b. In both these cases the calculated XUV signal shapes coincide remarkably well with those observed in a real experiment, as illustrated by Fig. 6c and 7c (cf. also [11]).

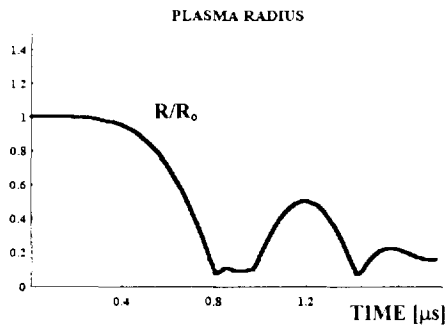


Fig. 6a

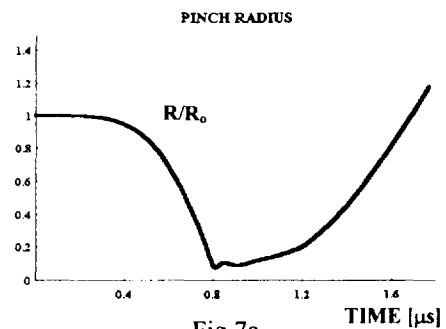


Fig. 7a

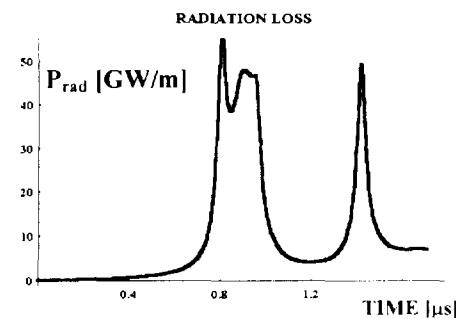


Fig. 6b

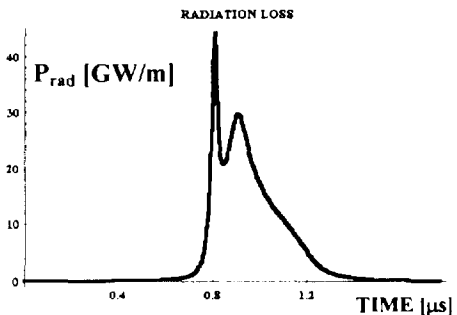


Fig. 7b

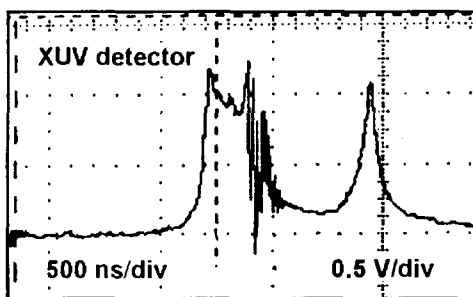


Fig. 6c

XUV diode signal at a fast current disruption

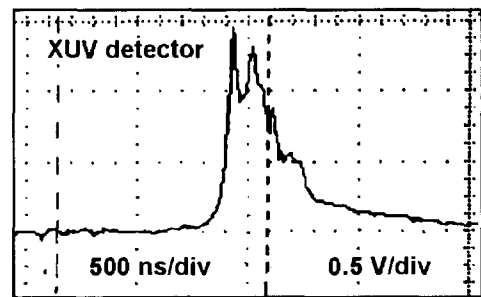


Fig. 7c

XUV diode signal at a slow current disruption

## Conclusion

The performed computations of a Z-pinch dynamics show that neither the Joule heating, nor the internal kinetic and magnetic (due to partially frozen driving magnetic field) pressures can stop the plasma radiation collapse, if full radiation losses are taken into account.

Contrary, if the radiation losses are artificially reduced even the 1-D model gives realistic time dependencies of both plasma radius and temperature, and the values of the minimum plasma radius and maximum plasma temperature at the stage of the first plasma compression agree well with those obtained by using several independent methods of plasma diagnostics. The simulated curves make it possible to explain all the main features of the observed XUV signals, namely the repeated bouncing observed at non-optimum pinch parameters, and pronounced splitting of the radiation peak corresponding to the first plasma compression.

Experimental XUV signals in non-optimum pinching regimes witness, we believe, full or partial (reversible) disruption of the driving current occurring at the time of maximum plasma compression.

This work has been supported in part by the Grant Agency of the Czech Academy of Sciences under contracts No 14358 and A1043504

## References:

- [1] Krejčí, A. et al: Proc. 17th Symp. Plasma Ph. & Techn., Prague 1995, p. 107
- [2] Krejčí, A.: Czech. J. Phys. 40 (1990) 182
- [3] Jungwirth, K., Ullschmied, J.: IPPCZ-244 (1981) 144
- [4] Mosher, D.: Proc. AIP Conf. on Dense Z-Pinches, Laguna Beach 1989, p. 191, 262
- [5] Mosher, D., Colombant, D.: Phys.Rev.Letters 68 (1992) 2600
- [6] Miyamoto, T., et al: Proc. AIP Conf. on Dense Z-Pinches, Laguna Beach 1989, p. 447
- [7] Breton, C., de Michelis, C., Mattioli, M.: Jour. Quant. Spectr. Rad., 19 (1978) 367
- [8] Cox, P.D., Tucker, W.H.: The Astrophys. Journal, 157 (1969) 1157
- [9] Drawin, W.H. in: At. and Mol. Data for Fusion, IAEA Vienna-199 (1977) 217
- [10] Krejčí, A., Krouský, E., Renner, O.: Czech J. Phys. 40 (1990) 1244
- [11] Krejčí, A. et al.: Proc. BEAMS'94, May 25-29, Washington D.C., Vol. III, p. 2020